

A modified micrometeorological gradient method for estimating O₃ dry deposition over a forest canopy

Zhiyong Wu¹, Leiming Zhang¹, Xuemei Wang², J. William Munger³

¹Air Quality Research Division, Science and Technology Branch, Environment Canada, Toronto, Canada

²School of Environmental Science and Engineering, Sun Yat-sen University, Guangzhou, China

³School of Engineering and Applied Sciences and Department of Earth and Planetary Sciences, Harvard University, Cambridge, Massachusetts, USA

Correspondence to: L. Zhang (leiming.zhang@ec.gc.ca)

1 **Abstract:** Small pollutant concentration gradients between levels above a plant
2 canopy result in large uncertainties in estimated air-surface exchange fluxes when
3 using existing micrometeorological gradient methods, including the aerodynamic
4 gradient method (AGM) and the modified Bowen-Ratio method (MBR). A modified
5 micrometeorological gradient method (MGM) is proposed in this study for estimating
6 O₃ dry deposition fluxes over a forest canopy using concentration gradients between a
7 level above and a level below the canopy top, taking advantage of relatively large
8 gradients between these levels due to significant pollutant uptake at top layers of the
9 canopy. The new method is compared with the AGM and MBR methods and is also
10 evaluated using eddy-covariance (EC) flux measurements collected at the Harvard
11 Forest Environmental Measurement Site, Massachusetts during 1993-2000. All the
12 three gradient methods (AGM, MBR and MGM) produced similar diurnal cycles of
13 O₃ dry deposition velocity ($V_d(O_3)$) to the EC measurements, with the MGM method
14 being the closest in magnitude to the EC measurements. The multi-year average $V_d(O_3)$
15 differed significantly between these methods, with the AGM, MBR and MGM
16 method being 2.28, 1.45 and 1.18 times of that of the EC. Sensitivity experiments
17 identified several input parameters for the MGM method as first-order parameters that
18 affect the estimated $V_d(O_3)$. A 10% uncertainty in the wind speed attenuation
19 coefficient or canopy displacement height can cause about 10% uncertainty in the
20 estimated $V_d(O_3)$. An unrealistic leaf area density vertical profile can cause an
21 uncertainty of a factor of 2.0 in the estimated $V_d(O_3)$. Other input parameters or
22 formulas for stability functions only caused an uncertainty of a few percent. The new

1 method provides an alternative approach in monitoring/estimating long-term
2 deposition fluxes of similar pollutants over tall canopies.

3

4 **1. Introduction**

5 Quantifying atmospheric dry and wet deposition of critical pollutants is important in
6 assessing their life time in air and their potential impact on various ecosystems. In
7 chemical transport models and in monitoring networks, dry deposition is commonly
8 estimated using the so-called inferential method, which requires a parameter - dry
9 deposition velocity (V_d) typically calculated using empirically developed dry
10 deposition algorithms (Wesely and Hicks, 2000; Pleim and Ran, 2011). Existing dry
11 deposition algorithms have large uncertainties, e.g., a factor of 2.0 on long-term basis
12 for several commonly studied species (Flechard et al., 2011; Schwede et al., 2011; Wu
13 et al., 2011; Wu et al., 2012; Matsuda et al., 2006). Field flux measurements are still
14 needed to reduce these uncertainties.

15 Measurements of O₃ dry deposition flux mostly rely on micrometeorological
16 methods (Wesely and Hicks, 2000). Two types of methods are commonly used: the
17 eddy-covariance technique and the flux-gradient methods. Eddy-covariance (EC) is a
18 direct measurement method determining turbulent fluxes without application of any
19 empirical assumption (Baldocchi et al., 1988; Stella et al., 2012). It has been
20 extensively used to estimate turbulent fluxes of momentum, heat, and trace gases (e.g.,
21 CO₂, H₂O, SO₂, O₃) (Baldocchi et al., 2001; Turnipseed et al., 2009; Guenther et al.,
22 2011). However, application of EC is often limited by the difficulty of making

1 high-quality measurements at sufficiently high frequencies (i.e. >1 Hz) to resolve the
2 covariance between vertical wind velocity and scalar concentration fluctuation (Jacob,
3 1999). Besides, EC method is costive and complex for maintenance.

4 A flux-gradient theory approach, also known as *K*-theory, was used as an
5 alternative method to determine fluxes of gases which lack the fast response
6 instrument for the EC measurement (Meyers et al., 1996; Park et al., 2014).
7 Flux-gradient theory assumes that the turbulence flux is proportional to the product of
8 the mean vertical concentration gradient and an eddy diffusivity (*K*) (Baldocchi et al.,
9 1988). The derivation of eddy diffusivity for air pollutants currently relies on the
10 similarity assumption which needs more verification from field measurements.
11 Another critical aspect when employing the flux-gradient theory is to measure the
12 concentrations of gases at different heights with sufficient accuracy and precision
13 (Stella et al., 2012; Loubet et al., 2013). Usually measurements at two adjacent levels
14 above a canopy are used to derive the gradient, e.g., the aerodynamic gradient method
15 (AGM) and the modified Bowen-Ratio approach (MBR). Due to the small
16 concentration gradient above the canopy and the instrument measurement
17 uncertainties, using the flux-gradient method can cause larger uncertainties in
18 estimated dry deposition fluxes.

19 On the other hand, gradients between levels above and below the canopy top are
20 usually sufficiently large due to the significant sink at top layers of forest canopies.
21 Thus, if concentration gradients at levels above and below the canopy top can be used
22 for estimating dry deposition flux, the uncertainties might be smaller. The present

1 study aims to develop and evaluate such a method (hereafter referred to as the
2 modified gradient method - MGM). It should be noted that this method is still based
3 on the flux-gradient theory.

4 Long-term concurrent measurements of eddy-covariance fluxes and
5 concentration profiles for O₃ and CO₂ have been conducted at the Harvard Forest
6 Environmental Measurement Site (HFEMS) since 1990 (Munger et al., 1996;
7 Urbanski et al., 2007). This data set enables us to estimate O₃ dry deposition using
8 existing (AGM, MBR and EC) and newly proposed (MGM) methods and thus to
9 evaluate the applicability and uncertainties in all the methods. The
10 micrometeorological methods are briefly described in Section 2, the measurement
11 data in Section 3, comparison results and sensitivity tests in Section 4, and major
12 conclusions and recommendations in Section 5.

13

14 **2. Micrometeorological methods of O₃ flux measurement**

15 *2.1. Eddy-covariance technique (EC)*

16 EC determines the turbulent flux (F) by calculating the covariance between vertical
17 wind velocity (w) and concentration of the gas (c):

$$18 \quad F = \overline{w'c'} \quad (1)$$

19 where the over-bar denotes the time average and the primes denote fluctuations from
20 the mean ($x' = x(t) - \bar{x}$, \bar{x} = mean). By convention, a positive flux is upward
21 (emission) and negative flux is downward (deposition).

22

2.2. Aerodynamic gradient method (AGM)

With an assumption that turbulent transport is analogous to molecular diffusion (Baldocchi et al., 1988), the flux-gradient theory is theoretically described as follows:

$$F = -K_c(z) dC/dz \quad (2)$$

where K_c is the eddy diffusivity for the gas, and dC/dz is the vertical concentration gradient of the gas. Two of the more popular methods for calculating K_c are the aerodynamic gradient method (AGM) and the modified Bowen-Ratio approach (MBR).

The AGM method assumes that heat and mass are transported in a similar way within a well-developed surface layer (Erisman and Draaijers, 1995). K_c is related to the interstitial aerodynamic resistance (R_a) (Baldocchi, 1988) as

$$R_a(z_1 : z_2) = \int_{z_2}^{z_1} dz / K_c(z) \quad (3)$$

where z_1 and z_2 indicate the heights of adjacent levels above canopy ($z_1 > z_2$).

Using Eqs. (2) and (3), the deposition flux (F) is determined as:

$$F = -\frac{\Delta C}{R_a(z_1 : z_2)} = -\frac{C_1 - C_2}{R_a(z_1 : z_2)} \quad (4)$$

where C_1 and C_2 indicate the gas concentrations at z_1 and z_2 , respectively.

R_a is calculated as

$$R_a(z_1 : z_2) = (\kappa u_*^{-1}) \left[\ln \frac{z_1 - d}{z_2 - d} + \psi_h \left(\frac{z_1 - d}{L} \right) - \psi_h \left(\frac{z_2 - d}{L} \right) \right] \quad (5)$$

where κ is the von Karman's constant (0.4), u_* the friction velocity ($u_* \equiv (-\overline{u'w'})^{1/2}$) measured at the reference height, d the zero-plane displacement height, L the Obukhov length, and Ψ_h the integrated stability correction function for heat using

1 those proposed by Businger et al. (1971) and modified by Högström (1988).

2

3 *2.3. Modified Bowen-Ratio method (MBR)*

4 The MBR method is also based on the flux-gradient theory (Eq. 2), but the eddy
5 diffusivity (K_c) is derived from flux and gradient measurements of another scalar (e.g.,
6 sensible heat, CO₂, H₂O) and assumes it is equal to K_c of the gas of interest. In this
7 study, the flux and gradient measurements of CO₂ are available at the same heights of
8 O₃, so K_c of O₃ was calculated from the CO₂ measurements as follows:

$$9 \quad K_c = K_{co_2} = -F_{co_2} \Delta z / \Delta C(CO_2) \quad (6)$$

10 where K_{co_2} is the eddy diffusivity of CO₂, F_{co_2} is the eddy-covariance flux of CO₂,
11 $\Delta C(CO_2)$ is the concentration gradient of CO₂ over the same height interval as
12 $\Delta C(O_3)$, and Δz is the height interval of concentration measurements.

13 Using Eqs. (2) and (6), the O₃ flux (F) is calculated as:

$$14 \quad F = F_{co_2} \Delta C(O_3) / \Delta C(CO_2) \quad (7)$$

15

16 *2.4. Modified gradient method (MGM)*

17 The newly proposed MGM method is also based on the flux-gradient theory (Eq. 2). It
18 is noted that the flux-gradient theory has been long questioned within plant canopy
19 environment due to infrequent but predominant large eddies within canopy (Wilson,
20 1989; Raupach, 1989). For example, Bache (1986) suggested that the flux-gradient
21 theory was a reasonable assumption estimating wind profiles in the upper portion of
22 canopy, but failed to reproduce the secondary wind maximum that was often observed

1 within the trunk space of forests. It should also be noted that most of the O₃ uptake
 2 occurs in the upper layers of the canopy where most canopy leaves grow. Within these
 3 upper layers the vertical length scales of turbulence are probably smaller than the
 4 distance associated with changes in concentration and wind speed gradients
 5 (Baldocchi, 1988). Thus, the flux-gradient theory is likely applicable for estimating
 6 vertical flux distribution of air pollutants within a plant canopy, as has been used in
 7 previous studies (e.g., Baldocchi, 1988; Bash et al., 2010; Wolfe and Thornton, 2011).

8 Applying the flux-gradient theory within the canopy, a height-dependent flux
 9 ($F(z)$) can then be calculated as:

$$10 \quad F(z) = -K_c(z) \frac{dC}{dz} \quad (8)$$

11 where $z \leq h$, and $K_c(z)$ is the vertical eddy diffusivity. Based on Eq. (8), the O₃ flux at
 12 canopy top ($F(h)$) is defined as

$$13 \quad F(h) = -\frac{C_h - C_3}{R_a(h:z_3)} \quad (9)$$

14 where C_h and C_3 are the concentrations at canopy top (h) and the height of z_3 ($z_3 < h$),
 15 respectively. $R_a(h:z_3)$ is related to K_c as

$$16 \quad R_a(h:z_3) = \int_{z_3}^h dz / K_c(z) \quad (10)$$

17 According to the aerodynamic gradient method (Eq. 4), the O₃ flux above canopy
 18 can be calculated from the concentration gradient between the reference height z_1 and
 19 the canopy top h ($z_1 > h$) as follows:

$$20 \quad F = -\frac{C_1 - C_h}{R_a(z_1:h)} \quad (11)$$

21 And based on the assumption of a constant flux layer above the canopy, the O₃ flux

1 above the canopy calculated in Eq. (11) should be equal to the O_3 flux at the canopy
 2 top derived from Eq. (9). Using Eqs. (9) and (11), we can derive that:

$$3 \quad F = -\frac{C_1 - C_3}{R_a(z_1 : h) + R_a(h : z_3)} \quad (12)$$

4 $R_a(z_1 : h)$ is calculated using Eq. (5). $R_a(h : z_3)$ is integrated vertically between
 5 the two heights within the canopy using Eq. (10).

6 $K_c(z)$ is assumed to equal $0.8K_m(z)$, which is the within canopy eddy diffusivity
 7 for momentum transfer (Halldin and Lindroth, 1986). As described in Baldocchi
 8 (1988), $K_m(z)$ is determined as

$$9 \quad K_m(z) = \frac{\int_0^z C_m(z) a(z) u(z)^2 dz}{du(z)/dz} \quad (13)$$

10 where $a(z)$ is the leaf area density at height z , and $u(z)$ is the horizontal wind speed
 11 within canopy. Similar to Baldocchi (1988), $K_m(z)$ is assumed to be constant below
 12 crown closure (about $0.7h$) and equal to K_m at $0.7h$. Thus we suggest here that the
 13 level of concentration measurement below canopy (z_3) should not be lower than the
 14 crown closure of canopy.

15 The effective drag coefficient ($C_m(z)$) is assumed to be constant with height (see
 16 Thom, 1975) following Baldocchi (1988):

$$17 \quad C_m(z) = \frac{C_{am}}{LAI [u_m/u(z_1)]^2} \quad (14)$$

18 where LAI is the canopy leaf area index, u_m the mean wind speed within canopy, and
 19 $u(z_1)$ the wind speed at the reference height z_1 . The bulk canopy drag coefficient (C_{am})
 20 is computed as

$$21 \quad C_{am} = u_*^2 / u(z_1)^2 \quad (15)$$

1 The mean within canopy wind speed (u_m) is calculated as

$$2 \quad u_m = (1/h) \int_0^h u(z) dz \quad (16)$$

3 Within canopy wind speed profile ($u(z)$) follows Cionco (1972):

$$4 \quad u(z) = u_h e^{-\alpha(1-z/h)} \quad (17)$$

5 where u_h is wind speed at the canopy top, and α is wind speed attenuation coefficient.

6 The above canopy logarithmic wind profile is used to scale the wind speed measured
7 at the reference height z_1 to the canopy height h :

$$8 \quad u_h = u(z_1) \frac{\ln(h-d) - \ln(z_0) + \psi_m \left[\frac{(h-d)}{L} \right] - \psi_m \left[\frac{z_0}{L} \right]}{\ln(z_1-d) - \ln(z_0) + \psi_m \left[\frac{(z_1-d)}{L} \right] - \psi_m \left[\frac{z_0}{L} \right]} \quad (18)$$

9 where z_0 is the roughness length for momentum, and ψ_m is the integrated stability
10 correction function for momentum as proposed by Businger et al. (1971) and
11 modified by Högström (1988).

12 Assuming a zero concentration on the absorbing surface, the dry deposition
13 velocity (V_d) of O_3 can be determined as

$$14 \quad V_d = -F / C(z_1) \quad (19)$$

15 where $C(z_1)$ is the O_3 concentration measured at the reference height z_1 .

16

17 **3. Field measurements used in this study**

18 *3.1. Site description*

19 The Harvard Forest Environmental Measurement Site (HFEMS) (42.54 N, 72.18 W)
20 is located in central Massachusetts at an elevation of 340 m above sea level. The
21 forest is 80-year-old on average, which consists of red maple (*Acer rubrum*) and red

1 oak (*Quercus rubra*) with scattered stands of Eastern hemlock (*Tsuga canadensis*), red
2 pine (*Pinus resinosa*) and white pine (*Pinus strobus*). The canopy height near the
3 observation tower is up to 23 m with a peak leaf area index (*LAI*) of $\sim 5.0 \text{ m}^2 \text{ m}^{-2}$
4 during summer. The nearest sources of significant pollution are a secondary road
5 about 2 km to the west of the site and a main highway about 5 km to the north.

6 A permanent 30-m Rohn 25G tower has been utilized at HFEMS to measure
7 eddy-covariance fluxes of sensible heat, H_2O , momentum, CO_2 , and O_3 , along with
8 vertical profiles of CO_2 and O_3 since 1990 (Fig. 1). Eddy-covariance fluxes were
9 measured at a height of 29 m above the ground. For the profile measurements air was
10 continuously sampled from heights of 29, 24.1, 18.3, 12.7, 7.5, 4.5, 0.8, and 0.3 m
11 AGL to determine the concentrations of CO_2 and O_3 . In this study, the upper three
12 levels were used to derive the gradients. Details on the site and the instrumental
13 methods can be found in Munger et al. (1996). Data used in this study are available
14 online at <http://atmos.seas.harvard.edu/lab/data/nigec-data.html>.

15 Zhao et al. (2011) retrieved the vertical profile of leaf area density at Harvard
16 Forest from a ground-based lidar scanning. Two tree species groups (i.e. Hardwood
17 and Conifer) were chosen. According to the species composition around the
18 measurement tower, the average leaf area density used in this study was calculated as
19 75% of that of Hardwood and 25% of that of Conifer from Zhao et al. (2011), as
20 shown in Fig. 1.

21 The monthly averaged leaf area index (*LAI*) at HFEMS was derived from the
22 ground-based measurements for most years between 1998 and 2013 using the LICOR

1 LAI-2000 system at 30-40 plots around the tower (Urbanski et al., 2007). As the
2 measurements during January and February were not available, these values were
3 obtained based on extrapolation (Fig. 2). The roughness length (z_0) and displacement
4 height (d) were calculated as a function of canopy height (h) and LAI , following
5 Meyers et al. (1998) (see Fig. 2):

$$6 \quad z_0 = h(0.215 - LAI^{0.25} / 10) \quad (20)$$

$$7 \quad d = h(0.1 + LAI^{0.2} / 2) \quad (21)$$

8

9 *3.2. Data selection*

10 A total of 10,252 hourly measuring points, recorded at HFEMS during 1993-2000,
11 were screened to eliminate the influence of periods associated with instrumental and
12 measurement problems and violation of the use of the flux-gradient theory.

13 In order to reduce the random measurement error in the concentration gradient,
14 O_3 concentrations below 1 ppbv were rejected, resulting in approximately 0.1% of the
15 data being omitted. In addition, periods with $[O_3] < [NO_y]$ (1.9%) were excluded to
16 avoid periods when O_3 chemical reactions may exceed O_3 deposition (Munger et al.,
17 1996). Wind speed below 1.0 m s^{-1} (1.2%) and drag coefficient below 0.02 (6.6%)
18 were removed because of probable invalid flux-gradient relationships (Feliciano et al.,
19 2001). Outliers in the data (2.9%) were removed, omitting any deposition velocity
20 exceeding the maximum achievable deposition velocity $V_{d,\max}$ ($V_{d,\max} = 1 / (R_a + R_b)$),
21 by more than a factor of 1.5 (Matsuda et al., 2006). Periods with counter-gradient
22 profiles (69.8%) which represent a downward flux (from EC measurement) while

1 with a negative gradient (upper level minus lower level) or vice versa were rejected
2 (Park et al., 2014). The counter-gradient transport should be mainly due to the
3 non-local nature of turbulent transport within canopies. Large sweep-ejection air
4 motions associated with coherent structures that can deeply penetrate into the canopy
5 are believed to be largely responsible for the exchange of momentum, heat and mass
6 between air above- and within-canopy (e.g, Shaw et al., 1983; Thomas and Foken,
7 2007). A total of 74.0% of the data was omitted in the following analysis. This
8 percentage value is slightly smaller than the sum of those from all the criteria due to
9 the overlap of some data points between the criteria.

10 Fig. 3 shows the mean diurnal cycles of O_3 concentration at different heights
11 derived from the original dataset and from the data after selection. The O_3
12 concentration increased during the early morning to reach a daily maximum of over
13 40 ppbv in the early afternoon and then decreased to ~30 ppbv at night. As shown in
14 Fig. 3a, the gradient between the two heights above canopy (i.e. 29 and 24.1 m) was
15 only about 0.4 ppbv on average, smaller than that between the levels above canopy
16 (24.1 m) and inside canopy (18.3 m) (~0.8 ppbv). The gradients were relatively small
17 during the morning (e.g., 0.1 ppbv at 11 LST) compared to the other periods of the
18 day. In the morning, the most effective turbulent exchange between the air above- and
19 within-canopy would substantially reduce the gradients (Sörgel et al., 2011). It is
20 worth to mention that many earlier studies suggested that the effects of chemistry on
21 O_3 flux divergence in the near surface were generally small, likely because the
22 chemical reactions for O_3 have larger time scales than the turbulent transport (e.g.,

1 Gao et al., 1991; De Arellano and Duynkerke, 1992; Duyzer et al., 1997; Padro et al.,
2 1998; Stella et al., 2012). After screening the data with the criteria, the gradients
3 among these three levels were significantly larger, reaching up to 1.0 ppbv and 1.6
4 ppbv, respectively (see Fig. 3b).

5

6 **4. Results and Discussion**

7 *4.1 Comparison of $V_d(O_3)$ by the eddy-covariance and gradient methods*

8 O_3 dry deposition velocity ($V_d(O_3)$) measured by the eddy-covariance (EC) technique
9 at Harvard Forest typically ranged from 0.14-0.53 cm s^{-1} , with a median value of 0.30
10 cm s^{-1} during the study period (Table 1). Since the screened deposition velocities still
11 include certain outlying data, the mean value was calculated using data between 10th
12 and 90th percentiles in order to reduce the influence of the outlying data. Following
13 this approach, the mean $V_d(O_3)$ by the EC technique was 0.34 cm s^{-1} , which was
14 significantly smaller than those by the gradient methods (Table 1). The ratios of mean
15 $V_d(O_3)$ by the modified gradient (MGM), modified Bowen-Ratio (MBR), and
16 aerodynamic gradient (AGM) methods to that by the EC technique were 1.18, 1.45
17 and 2.28, respectively. Previous studies on the inter-comparisons of these methods for
18 O_3 are few and the results varied. Muller et al. (2009) found that the mean $V_d(O_3)$ by
19 the AGM method was 1.60-3.47 times those by the EC technique at a grassland in
20 Southern Scotland. Loubet et al. (2013) showed that the AGM method gave 40%
21 larger $V_d(O_3)$ than the EC technique over a mature maize field in Paris. Keronen et al.
22 (2003) found that $V_d(O_3)$ by the AGM and EC methods generally agreed well at a

1 Nordic pine forest, and so did Stella et al. (2012) over a bare soil in Paris. Droppo
2 (1985) found close $V_d(O_3)$ values with the MBR and EC methods at a Northeastern
3 U.S. grassland site.

4 Fig. 4 shows the diurnal cycles of $V_d(O_3)$ by the EC and gradient methods.
5 Although the trends were similar, the MBR and AGM $V_d(O_3)$ were consistently larger
6 than the EC $V_d(O_3)$. The EC $V_d(O_3)$ was about 0.2 cm s^{-1} on average during night and
7 reached a daily maximum of 0.5 cm s^{-1} around noon. The $V_d(O_3)$ by the MBR and
8 AGM methods reached around 0.8 and 1.3 cm s^{-1} during the daytime, respectively and
9 remained about 0.4 cm s^{-1} during night. The MGM $V_d(O_3)$ agreed well with the EC
10 $V_d(O_3)$ during the daytime but was slightly larger at night. This discrepancy has been
11 identified in previous studies (Keronen et al., 2003; Stella et al., 2012) and could be
12 due to the fact that nocturnal conditions affect both EC and gradient measurements.
13 The EC technique is found to underestimate flux during calm night-time periods at
14 Harvard Forest (Goulden et al., 1996). The stability correction functions used in the
15 gradient methods (AGM and MGM) are subject to large uncertainties under stable
16 conditions (Högström, 1988).

17 The very large differences in $V_d(O_3)$ between the AGM and EC methods should
18 be caused by a combination of various factors. As can be seen from Eq. (4), any
19 underestimation in the calculation of aerodynamic resistance (R_a) would directly
20 transfer to the overestimation of V_d . Uncertainties in R_a from using different formulas
21 are generally on the order of 30% over a whole canopy (Zhang et al., 2003). In the
22 case of Eq. (4), uncertainties can be larger than 30% if other uncertainties from the

1 related parameters are larger. The potential underestimation in R_a (Eq. 4) also explains
2 the small overestimation in V_d from the MGM method, in which the same R_a formula
3 is used, although plays a second role. Measurement uncertainties in concentration
4 gradients could also cause big discrepancies between the AGM and EC methods,
5 especially under small gradient conditions. This is supported by the finding that the
6 MBR method also overestimated V_d when compared with the EC measurements.

7 As shown in Fig. 5, the EC $V_d(O_3)$ exhibited a significant seasonal pattern with
8 peak values in summer ($\sim 0.5 \text{ cm s}^{-1}$) and small values in winter ($0.15\text{-}0.28 \text{ cm s}^{-1}$).
9 Both the MGM and MBR methods captured this seasonal cycle, but the MGM method
10 produced a higher $V_d(O_3)$ than the EC technique during winter (December-February)
11 and the MBR method gave a significant overestimation in summer (June-September).
12 The monthly AGM $V_d(O_3)$ was consistently larger than the EC $V_d(O_3)$ and exhibited a
13 less clear seasonal pattern with alternating increases and decreases in the $V_d(O_3)$.

14

15 *4.2 Sensitivity of $V_d(O_3)$ by the modified gradient method to the key* 16 *parameters/formulas*

17 As shown in Section 4.1, the MGM method performed better than the MBR and AGM
18 methods. This improvement should mainly be attributed to reductions in errors of O_3
19 concentration gradients. However, the MGM method increased the complexity in the
20 algorithm and added more model parameters, which may in turn increase the
21 uncertainty in the estimated $V_d(O_3)$.

22 To test the sensitivity of the estimated $V_d(O_3)$ by the MGM method to the key

1 parameters/formulas, calculations were conducted by changing the
2 parameters/formulas within a reasonable range. For some single-value parameters (i.e.
3 roughness length, displacement height, wind speed attenuation coefficient, and leaf
4 area index), sensitivity tests were conducted by increasing or decreasing the value by
5 10%.

6 As shown in Fig. 6 and Table 2, the MGM $V_d(O_3)$ was highly sensitive to the
7 changes in wind speed attenuation coefficient and displacement height. Higher wind
8 speed attenuation coefficient could result in lower within-canopy wind speed (Eq. 17)
9 and thus lower eddy exchange coefficient and $V_d(O_3)$ (Table 2). Based on a
10 least-square fitting of within-canopy wind profiles measured at Harvard Forest for
11 noon-periods in summer, the attenuation coefficient was estimated to be ~ 10.6 at
12 Harvard Forest. Cionco (1972) suggested that the attenuation coefficient varies with
13 leaf area. Therefore, the application of this value throughout the whole year could
14 produce a certain uncertainty in the estimated $V_d(O_3)$.

15 The MGM $V_d(O_3)$ increased when the displacement height increased or vice
16 versa (Fig. 6, Table 2). Sakai et al. (2001) calculated the displacement height at
17 Harvard Forest using noon-period measurements and indicated the ratio of
18 displacement height to canopy height was 0.77 in summer with foliated canopy and
19 0.6 in winter with leafless canopy. In this study, we estimated a close value in summer
20 (0.79) and a slightly higher value in winter (0.66) using the method proposed by
21 Meyers et al. (1998) (Fig. 2). The overestimation of the displacement height could
22 partly explain the overestimation of $V_d(O_3)$ by the MGM method during December to

1 February (Fig. 5).

2 Fig. 6 shows that the MGM $V_d(O_3)$ was less sensitive to the changes of
3 roughness length and leaf area index. The relative differences in the estimated $V_d(O_3)$
4 were less than 2% when roughness length and leaf area index varied by 10% (Table
5 2).

6 Meyers et al. (1998) provided three typical types of leaf area density profiles,
7 which are significantly different in shape from the profile in Harvard Forest used in
8 this study (see Fig. 7). We conducted sensitivity experiments by replacing the Harvard
9 Forest profile with those in Meyers et al. (1998) to assess the impact of vertical profile
10 of leaf area density on the determination of $V_d(O_3)$. As shown in Fig. 6 and Table 2,
11 the vertical profile of leaf area density impacted the estimated $V_d(O_3)$ greatly, with a
12 relative difference in $V_d(O_3)$ of above 50%. The profile with higher leaf density in the
13 upper canopy (profile 3) resulted in a higher $V_d(O_3)$ while the profile with abundant
14 understory plants (profile 1) led to a lower $V_d(O_3)$.

15 In this study, the stability correction functions proposed by Businger et al. (1971)
16 and modified by Högström (1988) were used, but several others exist, such as those
17 by Dyer (1974), Paulson (1970), and Webb (1970). Fig. 6 indicated that uncertainties
18 in the stability correction functions for heat (Ψ_h) and momentum (Ψ_m) had little
19 impact on the MGM $V_d(O_3)$ values. The relative difference of V_d was less than 4% for
20 different Ψ_h and less than 1% for different Ψ_m . Stella et al. (2012) found that the
21 variation of $V_d(O_3)$ on different Ψ_h was roughly 10% on average when using the AGM
22 method. Ψ_h influences the estimation of V_d due to the impact on the calculation of

1 turbulent transfer above the canopy. As the MGM method considered both the above-
2 and within- canopy turbulence transfer, the MGM $V_d(O_3)$ values were thus less
3 sensitive to the choice of Ψ_h .

4

5 **5. Conclusions and Recommendations**

6 A modified micrometeorological gradient method was developed to quantify O_3 dry
7 deposition over a forest canopy making use of concentration gradients between levels
8 above and below the canopy top. The MGM method produced close $V_d(O_3)$ to the
9 eddy-covariance measurements at Harvard Forest during daytime, although slightly
10 overestimated the measurements at night. The modified method seemed to be an
11 improvement compared to the two existing flux-gradient methods (AGM and MBR)
12 in terms of predicted long-term mean, diurnal and seasonal cycles of $V_d(O_3)$.
13 Sensitivity tests show that model parameters for MGM including wind speed
14 attenuation coefficient, canopy displacement height and vertical distribution of leaf
15 density were first-order parameters affecting the estimated $V_d(O_3)$. Model results were
16 less sensitive to roughness length, leaf area index, and stability function for heat and
17 momentum.

18 The newly-developed MGM method has potential to be applied routinely to
19 monitor/estimate long-term deposition fluxes of O_3 and other similar pollutants over
20 tall canopies. The within-canopy measurement should be close to but not lower than
21 the canopy closure height where most of the flux exchange occurs. Key model
22 parameters mentioned above need to be characterized as accurate as possible. For

1 example, seasonal profiles of vertical distribution of leaf area density, canopy
2 displacement height, and vertical wind profile related parameters are needed.

3

4 **Acknowledgments**

5 This work is funded by the Clean Air and Regulatory Agenda program. X. Wang is
6 supported by the Natural Science Foundation of China (grant 41275018).

7

8 **References**

- 9 Bache, D. H.: Momentum transfer to plant canopies: influence of structure and
10 variable drag, *Atmos. Environ.*, 20, 1369-1378, 1986.
- 11 Baldocchi, D.: A multi-layer model for estimating sulfur dioxide deposition to a
12 deciduous oak forest canopy, *Atmos. Environ.*, 22, 869-884, 1988.
- 13 Baldocchi, D., Falge, E., Gu, L., Olson, R., Hollinger, D., Running, S., Anthoni, P.,
14 Bernhofer, C., Davis, K., and Evans, R.: FLUXNET: A new tool to study the
15 temporal and spatial variability of ecosystem-scale carbon dioxide, water vapor,
16 and energy flux densities, *B. Am. Meteorol. Soc.*, 82, 2415-2434, 2001.
- 17 Baldocchi, D. D., Hincks, B. B., and Meyers, T. P.: Measuring biosphere-atmosphere
18 exchanges of biologically related gases with micrometeorological methods,
19 *Ecology*, 69, 1331-1340, 1988.
- 20 Bash, J. O., Walker, J. T., Katul, G. G., Jones, M. R., Nemitz, E., and Robarge, W. P.:
21 Estimation of in-canopy ammonia sources and sinks in a fertilized Zea Mays
22 field, *Environ. Sci. Technol.*, 44, 1683-1689, 2010.
- 23 Businger, J. A., Wyngaard, J. C., Izumi, Y., and Bradley, E. F.: Flux-profile

1 relationships in the atmospheric surface layer, *J. Atmos. Sci*, 28, 181-189, 1971.

2 Cionco, R. M.: A wind-profile index for canopy flow, *Bound.-Lay. Meteorol.*, 3,
3 255-263, 1972.

4 De Arellano, J. V. G. and Duynkerke, P. G.: Influence of chemistry on the
5 flux-gradient relationships for the NO-O₃-NO₂ system, *Bound.-Lay. Meteorol.*,
6 61, 375–387, 1992.

7 Droppo, J. G.: Concurrent measurements of ozone dry deposition using eddy
8 correlation and profile flux methods, *J. Geophys. Res.*, 90, 2111-2118, 1985.

9 Duyzer, J., Weststrate, H., Verhagen, H., Deinum, G., and Baak, J.: Measurements of
10 dry deposition fluxes of nitrogen compounds and ozone, in:
11 *Biosphere-atmosphere exchange of pollutants and trace substances:*
12 *Experimental and Theoretical Studies of Biogenic Emissions and Pollutant*
13 *Deposition*, edited by: Slanina, S., Springer, 4, 244–250, 1997.

14 Erisman, J. W., and Draaijers, G. P. J.: Atmospheric deposition in relation to
15 acidification and eutrophication, *Studies in environmental science*, 63, Elsevier,
16 Amsterdam, 64-66 pp., 1995.

17 Feliciano, M., Pio, C., and Vermeulen, A.: Evaluation of SO₂ dry deposition over
18 short vegetation in Portugal, *Atmos. Environ.*, 35, 3633-3643, 2001.

19 Flechard, C., Nemitz, E., Smith, R., Fowler, D., Vermeulen, A., Bleeker, A., Erisman,
20 J., Simpson, D., Zhang, L., and Tang, Y.: Dry deposition of reactive nitrogen to
21 European ecosystems: a comparison of inferential models across the NitroEurope
22 network, *Atmos. Chem. Phys.*, 11, 2703-2728, doi:10.5194/acp-11-2703-2011,

1 2011.

2 Gao, W., Wesely, M. L., and Lee, I. Y.: A numerical study of the effects of air
3 chemistry on fluxes of NO, NO₂, and O₃ near the surface, *J. Geophys.*
4 *Res.-Atmos.*, 96, 18761–18769, doi:10.1029/91JD02106, 1991.

5 Goulden, M. L., Munger, J. W., FAN, S. M., Daube, B. C., and Wofsy, S. C.:
6 Measurements of carbon sequestration by long-term eddy covariance: Methods
7 and a critical evaluation of accuracy, *Global Change Biol.*, 2, 169-182, 1996.

8 Guenther, A., Kulmala, M., Turnipseed, A., Rinne, J., SUN, T., and Reissell, A.:
9 Integrated land ecosystem-atmosphere processes study (iLEAPS) assessment of
10 global observational networks, *Boreal Environ. Res.*, 16, 321-336, 2011.

11 Högström, U.: Non-dimensional wind and temperature profiles in the atmospheric
12 surface layer: A re-evaluation, *Bound.-Lay. Meteorol.*, 42, 55-78, 1988.

13 Halldin, S., and Lindroth, A.: Pine forest microclimate simulation using different
14 diffusivities, *Bound.-Lay. Meteorol.*, 35, 103-123, 1986.

15 Jacob, D.: Introduction to atmospheric chemistry, Princeton University Press, New
16 Jersey, 64 pp., 1999.

17 Keronen, P., Reissell, A., Rannik, U., Pohja, T., Siivola, E., Hiltunen, V., Hari, P.,
18 Kulmala, M., and Vesala, T.: Ozone flux measurements over a Scots pine forest
19 using eddy covariance method: performance evaluation and comparison with
20 flux-profile method, *Boreal Environ. Res.*, 8, 425-444, 2003.

21 Loubet, B., Cellier, P., Fléchar, C., Zurfluh, O., Irvine, M., Lamaud, E., Stella, P.,
22 Roche, R., Durand, B., and Flura, D.: Investigating discrepancies in heat, CO₂

1 fluxes and O₃ deposition velocity over maize as measured by the
2 eddy-covariance and the aerodynamic gradient methods, *Agr. Forest Meteorol.*,
3 169, 35-50, 2013.

4 Matsuda, K., Watanabe, I., Wingpud, V., Theramongkol, P., and Ohizumi, T.:
5 Deposition velocity of O₃ and SO₂ in the dry and wet season above a tropical
6 forest in northern Thailand, *Atmos. Environ.*, 40, 7557-7564, 2006.

7 Meyers, T. P., Hall, M. E., Lindberg, S. E., and Kim, K.: Use of the modified
8 Bowen-ratio technique to measure fluxes of trace gases, *Atmos. Environ.*, 30,
9 3321-3329, 1996.

10 Meyers, T. P., Finkelstein, P., Clarke, J., Ellestad, T. G., and Sims, P. F.: A multilayer
11 model for inferring dry deposition using standard meteorological measurements,
12 *J. Geophys. Res.*, 103, 22645-22661, 1998.

13 Muller, J., Coyle, M., Fowler, D., Gallagher, M. W., Nemitz, E. G., and Percival, C.
14 J.: Comparison of ozone fluxes over grassland by gradient and eddy covariance
15 technique, *Atmos. Sci. Lett.*, 10, 164-169, 2009.

16 Munger, J. W., Wofsy, S. C., Bakwin, P. S., Fan, S. M., Goulden, M. L., Daube, B.
17 C., Goldstein, A. H., Moore, K. E., and Fitzjarrald, D. R.: Atmospheric
18 deposition of reactive nitrogen oxides and ozone in a temperate deciduous forest
19 and a subarctic woodland: 1. Measurements and mechanisms, *J. Geophys. Res.*,
20 101, 12639-12657, 1996.

21 Padro, J., Zhang, L., and Massman, W. J.: An analysis of measurements and
22 modelling of air-surface exchange of NO-NO₂-O₃ over grass, *Atmos. Environ.*,

- 1 32, 1365–1375, 1998.
- 2 Park, J.-H., Fares, S., Weber, R., and Goldstein, A. H.: Biogenic volatile organic
3 compound emissions during BEARPEX 2009 measured by eddy covariance and
4 flux–gradient similarity methods, *Atmos. Chem. Phys.*, 14, 231-244, 2014.
- 5 Pleim, J., and Ran, L.: Surface flux modeling for air quality applications, *Atmos.*, 2,
6 271-302, 2011.
- 7 Raupach, M.: A practical Lagrangian method for relating scalar concentrations to
8 source distributions in vegetation canopies, *Q. J. Roy. Meteor. Soc.*, 115,
9 609-632, 1989.
- 10 Sakai, R. K., Fitzjarrald, D. R., and Moore, K. E.: Importance of low-frequency
11 contributions to eddy fluxes observed over rough surfaces, *J. Appl. Meteorol.*,
12 40, 2178-2192, 2001.
- 13 Schwede, D., Zhang, L., Vet, R., and Lear, G.: An intercomparison of the deposition
14 models used in the CASTNET and CAPMoN networks, *Atmos. Environ.*, 45,
15 1337-1346, 2011.
- 16 Shaw, R. H., Tavangar, J., and Ward, D. P.: Structure of the Reynolds stress in a
17 canopy layer, *J. Clim. Appl. Met.*, 22(11), 1922-1931, 1983.
- 18 Sörgel, M., Trebs, I., Serafimovich, A., Moravek, A., Held, A., and Zetzsch, C.:
19 Simultaneous HONO measurements in and above a forest canopy: influence of
20 turbulent exchange on mixing ratio differences, *Atmos. Chem. Phys.*, 11,
21 841–855, doi:10.5194/acp-11-841-2011,15 2011.
- 22 Stella, P., Loubet, B., Laville, P., Lamaud, E., Cazaunau, M., Laufs, S., Bernard, F.,

- 1 Grosselin, B., Mascher, N., and Kurtenbach, R.: Comparison of methods for the
2 determination of NO-O₃-NO₂ fluxes and chemical interactions over a bare soil,
3 Atmos. Meas. Tech., 5, 1241-1257, doi:10.5194/amt-5-1241-2012, 2012.
- 4 Thom, A. S.: Momentum, mass and heat exchange of plant communities, in:
5 Vegetation and the Atmosphere, edited by: Monteith, J. L., Academic Press,
6 London, 57-109, 1975.
- 7 Thomas, C. and Foken, T.: Flux contribution of coherent structures and its
8 implications for the exchange of energy and matter in a tall spruce canopy,
9 Bound.-Lay. Meteorol., 123, 317–337, 2007.
- 10 Turnipseed, A. A., Burns, S. P., Moore, D. J., Hu, J., Guenther, A. B., and Monson, R.
11 K.: Controls over ozone deposition to a high elevation subalpine forest, Agr.
12 Forest Meteorol., 149, 1447-1459, 2009.
- 13 Urbanski, S., Barford, C., Wofsy, S., Kucharik, C., Pyle, E., Budney, J., McKain, K.,
14 Fitzjarrald, D., Czikowsky, M., and Munger, J.: Factors controlling CO₂
15 exchange on timescales from hourly to decadal at Harvard Forest, J. Geophys.
16 Res., 112, G02020, 2007.
- 17 Wesely, M., and Hicks, B.: A review of the current status of knowledge on dry
18 deposition, Atmos. Environ., 34, 2261-2282, 2000.
- 19 Wilson, J. D.: Turbulent transport within the plant canopy, in: Estimation of Areal
20 Evapotranspiration, edited by: Black, T. A., Spittlehouse, D. L., Novak, M. D.,
21 and Price, D. T., IAHS Press, Wallingford, UK, 43-80, 1989.
- 22 Wolfe, G. M. and Thornton, J. A.: The Chemistry of Atmosphere-Forest Exchange

1 (CAFE) Model – Part 1: Model description and characterization, *Atmos. Chem.*
2 *Phys.*, 11, 77–101, doi:10.5194/acp-11-77-2011, 2011.

3 Wu, Z. Y., Wang, X. M., Chen, F., Turnipseed, A. A., Guenther, A. B., Niyogi, D.,
4 Charusombat, U., Xia, B. C., Munger, J. W., and Alapaty, K.: Evaluating the
5 calculated dry deposition velocities of reactive nitrogen oxides and ozone from
6 two community models over a temperate deciduous forest, *Atmos. Environ.*, 45,
7 2663-2674, 2011.

8 Wu, Z. Y., Wang, X. M., Turnipseed, A. A., Chen, F., Zhang, L. M., Guenther, A. B.,
9 Karl, T., Huey, L. G., Niyogi, D., Xia, B. C., and Alapaty, K.: Evaluation and
10 improvements of two community models in simulating dry deposition velocities
11 for peroxyacetyl nitrate (PAN) over a coniferous forest, *J. Geophys. Res.*, 117,
12 12, 2012.

13 Zhang, L., Brook, J. R., and Vet, R.: Evaluation of a non-stomatal resistance
14 parameterization for SO₂ dry deposition, *Atmos. Environ.*, 37, 2941-2947, 2003.

15 Zhao, F., Yang, X., Schull, M. A., Román-Colón, M. O., Yao, T., Wang, Z., Zhang,
16 Q., Jupp, D. L., Lovell, J. L., and Culvenor, D. S.: Measuring effective leaf area
17 index, foliage profile, and stand height in New England forest stands using a
18 full-waveform ground-based lidar, *Remote Sens. Environ.*, 115, 2954-2964,
19 2011.

Figure Captions

1 Fig. 1. Schematic of flux and concentration gradient measurements at Harvard Forest
2 Environmental Measurement Site.

3

4 Fig. 2. Monthly variation of leaf area index (LAI), the displacement height (d) to
5 canopy height (h) ratio, and the roughness length (z_0) to canopy height ratio at
6 Harvard Forest.

7

8 Fig. 3. Mean diurnal cycles of O_3 concentration at heights of 29, 24.1, and 18.3 m
9 above ground level at Harvard Forest during 1993-2000. (a) was derived from the
10 original data, and (b) was from the data after selection.

11

12 Fig. 4. (a) The box-plot of hourly $V_d(O_3)$, and (b) diurnal average cycles of $V_d(O_3)$ at
13 Harvard Forest during 1993-2000 as measured by the eddy-covariance (EC) and three
14 gradient methods (MGM: the modified gradient method; MBR: the modified
15 Bowen-Ratio method; AGM: the aerodynamic gradient method). In each box, the
16 central mark is the median, and the edges of the box are the 10th and 90th percentiles.
17 Note that the average is the arithmetical mean of data between 10th and 90th
18 percentiles.

19

20 Fig. 5. Monthly average of $V_d(O_3)$ at Harvard Forest during 1993-2000 as measured
21 by the eddy-covariance (EC) and three gradient methods (MGM: the modified
22 gradient method; MBR: the modified Bowen-Ratio method; AGM: the aerodynamic
23 gradient method). Note that the average is the arithmetical mean of data between 10th

1 and 90th percentiles.

2

3 Fig. 6. Diurnal average cycles of $V_d(O_3)$ over Harvard Forest during 1993-2000 by the
4 modified gradient method (MGM) with different parameter/formula changes and
5 compared with that by the eddy-covariance (EC) technique: (a) roughness length, (b)
6 displacement height, (c) wind speed attenuation coefficient, (d) leaf area index, (e)
7 vertical profile of leaf area density, (f) stability correction functions for heat, and (g)
8 stability correction functions for momentum.

9

10 Fig. 7. Vertical profiles of leaf area density in Harvard Forest and those used in
11 sensitivity experiments.

12

13

14

15

16

17

18

19

20

21

22

23

Table 1. Statistics on hourly $V_d(O_3)$ (cm s^{-1}) at Harvard Forest during 1993-2000 as measured by the eddy-covariance (EC) and three gradient methods (MGM: the modified gradient method; MBR: the modified Bowen-Ratio method; AGM: the aerodynamic gradient method).

	EC	MGM	MBR	AGM
10 th Percentile	0.05	0.09	0.03	0.11
25 th Percentile	0.14	0.19	0.12	0.26
Median	0.30	0.35	0.35	0.62
75 th Percentile	0.53	0.61	0.85	1.27
90 th Percentile	0.83	0.96	1.86	2.28
Mean ^a	0.34	0.40	0.49	0.77

^a the arithmetical mean of data between 10th and 90th percentiles

Table 2. Relative difference between $V_d(O_3)$ determined by the modified gradient method with different parameters/formulas (%)^a

	z_0		d		α		LAI		LAD ^b			Ψ_h^c			Ψ_m^c		
	-10%	+10%	-10%	+10%	-10%	+10%	-10%	+10%	Prf 1	Prf 2	Prf 3	D74	P70	W70	D74	P70	W70
Median	-1.1	1.1	-4.8	10.8	10.1	-9.3	-0.6	0.5	-34.4	8.4	57.4	3.1	1.7	0.5	0.2	0.08	0.06
Mean ^d	-1.0	1.1	-4.7	10.4	10.2	-9.6	-0.6	0.5	-34.5	8.4	58.5	3.1	1.4	-0.01	0.1	0.02	-0.01

^a Relative difference = (Sensitivity – Base) / Base × 100%

^b Vertical profile of leaf area density from Meyers et al. (1998) as shown in Fig. 7

^c D74: Dyer (1974); P70: Paulson (1970); W70: Webb (1970)

^d the arithmetical mean of data between 10th and 90th percentiles

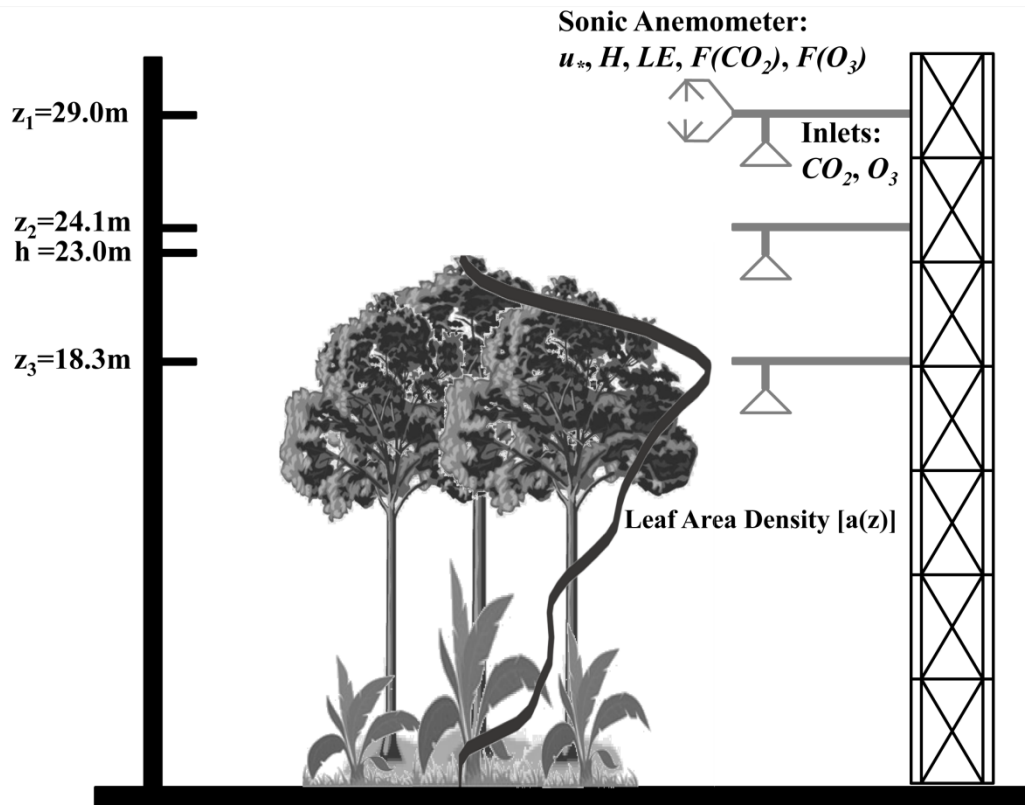


Fig. 1. Schematic of flux and concentration gradient measurements at Harvard Forest Environmental Measurement Site.

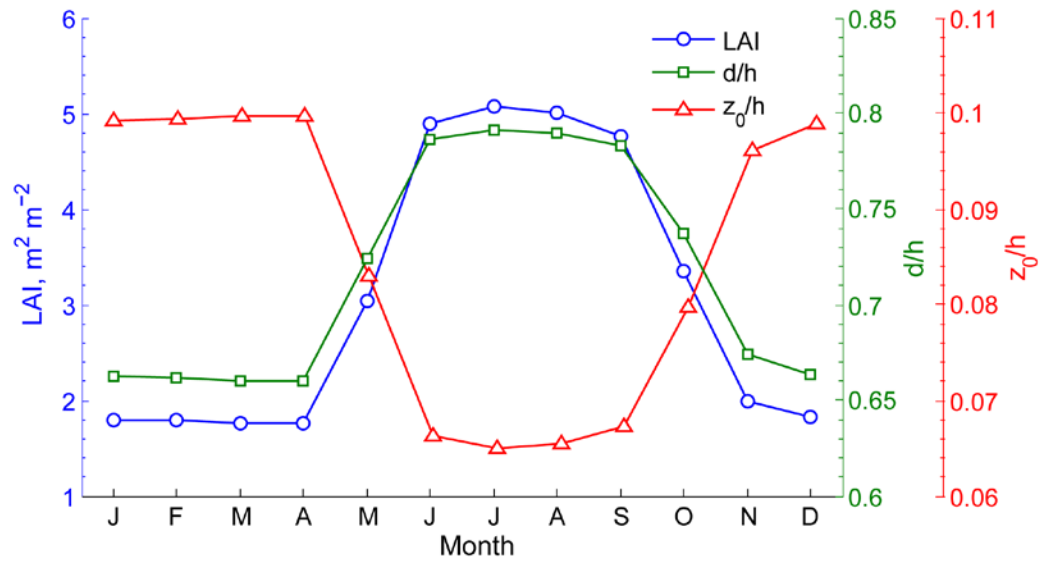


Fig. 2. Monthly variation of leaf area index (LAI), the displacement height(d) to canopy height (h) ratio, and the roughness length (z_0) to canopy height ratio at Harvard Forest.

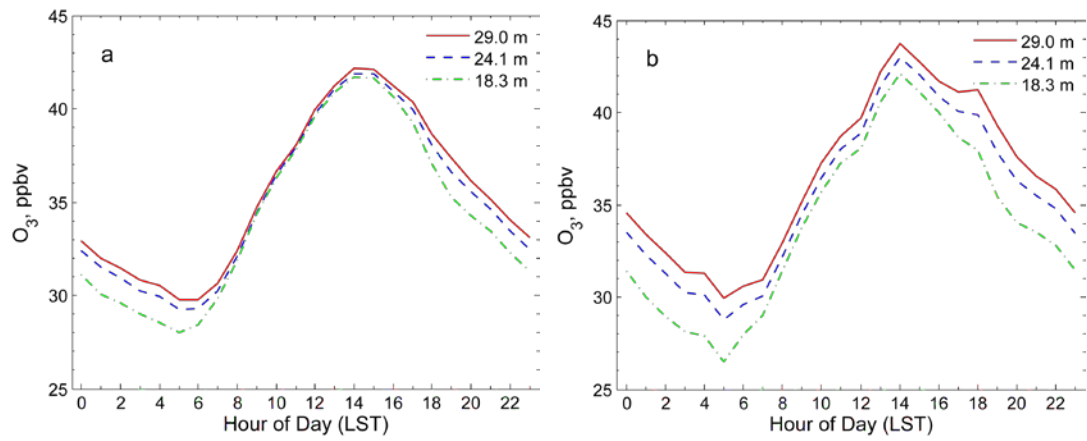


Fig. 3. Mean diurnal cycles of O_3 concentration at heights of 29, 24.1, and 18.3 m above ground level at Harvard Forest during 1993-2000. (a) was derived from the original data, and (b) was from the data after selection.

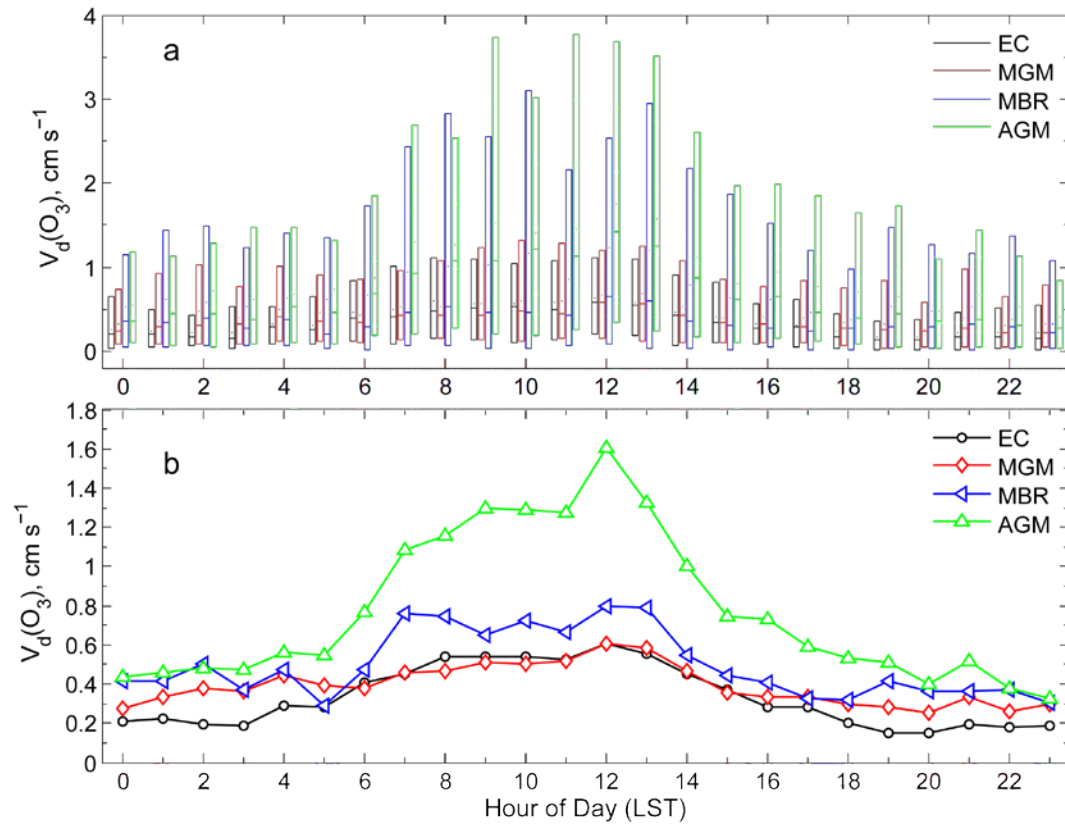


Fig. 4. (a) The box-plot of hourly $V_d(O_3)$, and (b) diurnal average cycles of $V_d(O_3)$ at Harvard Forest during 1993-2000 as measured by the eddy-covariance (EC) and three gradient methods (MGM: the modified gradient method; MBR: the modified Bowen-Ratio method; AGM: the aerodynamic gradient method). In each box, the central mark is the median, and the edges of the box are the 10th and 90th percentiles. Note that the average is the arithmetical mean of data between 10th and 90th percentiles.

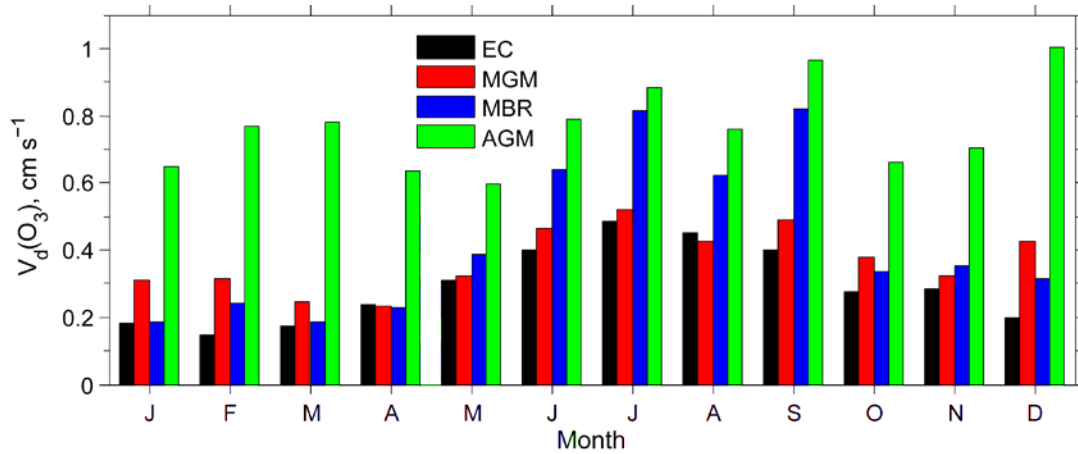


Fig. 5. Monthly average of $V_d(O_3)$ at Harvard Forest during 1993-2000 as measured by the eddy-covariance (EC) and three gradient methods (MGM: the modified gradient method; MBR: the modified Bowen-Ratio method; AGM: the aerodynamic gradient method). Note that the average is the arithmetical mean of data between 10th and 90th percentiles.

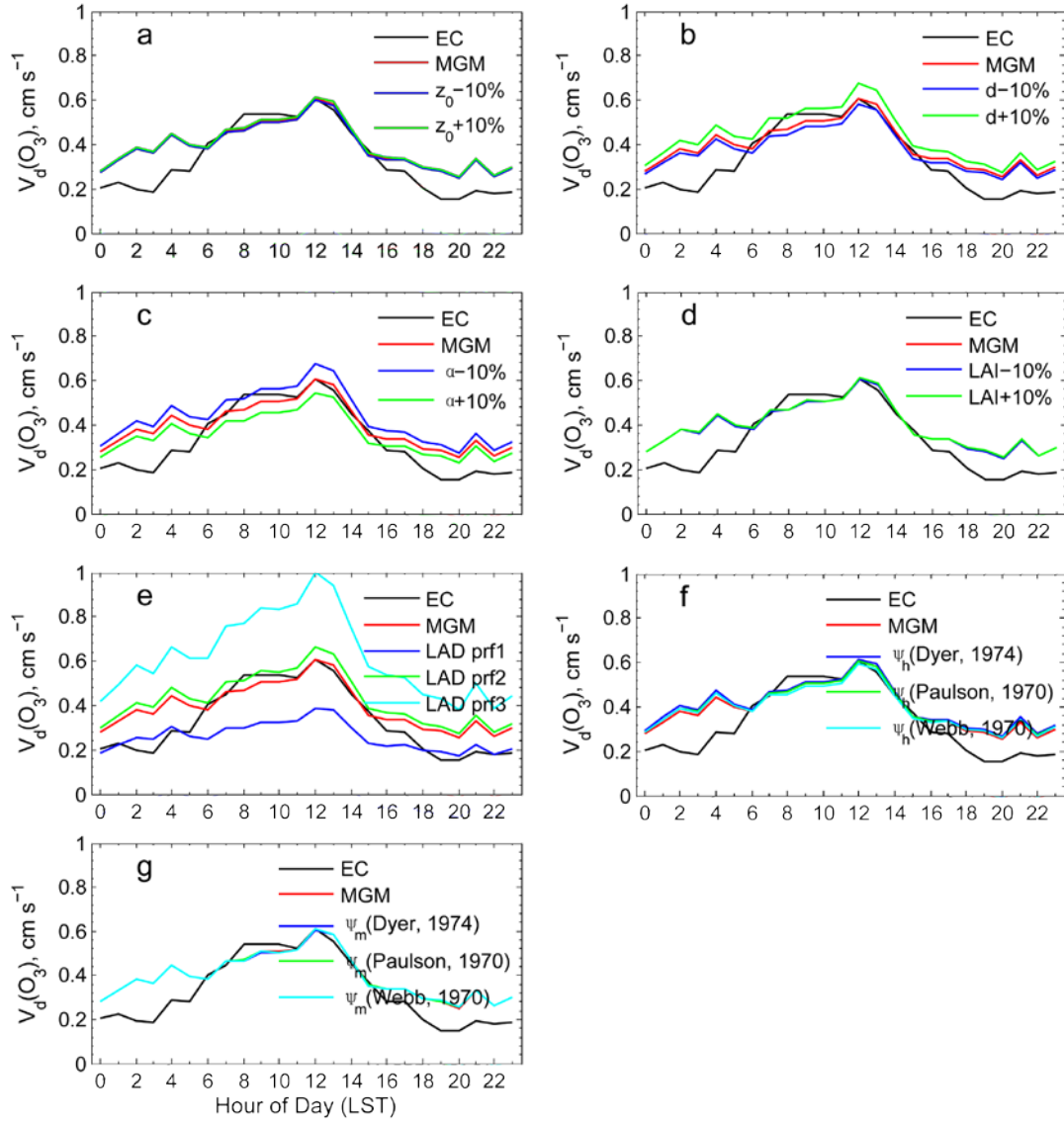


Fig. 6. Diurnal average cycles of $V_d(O_3)$ over Harvard Forest during 1993-2000 by the modified gradient method (MGM) with different parameter/formula changes and compared with that by the eddy-covariance (EC) technique: (a) roughness length, (b) displacement height, (c) wind speed attenuation coefficient, (d) leaf area index, (e) vertical profile of leaf area density, (f) stability correction functions for heat, and (g) stability correction functions for momentum.

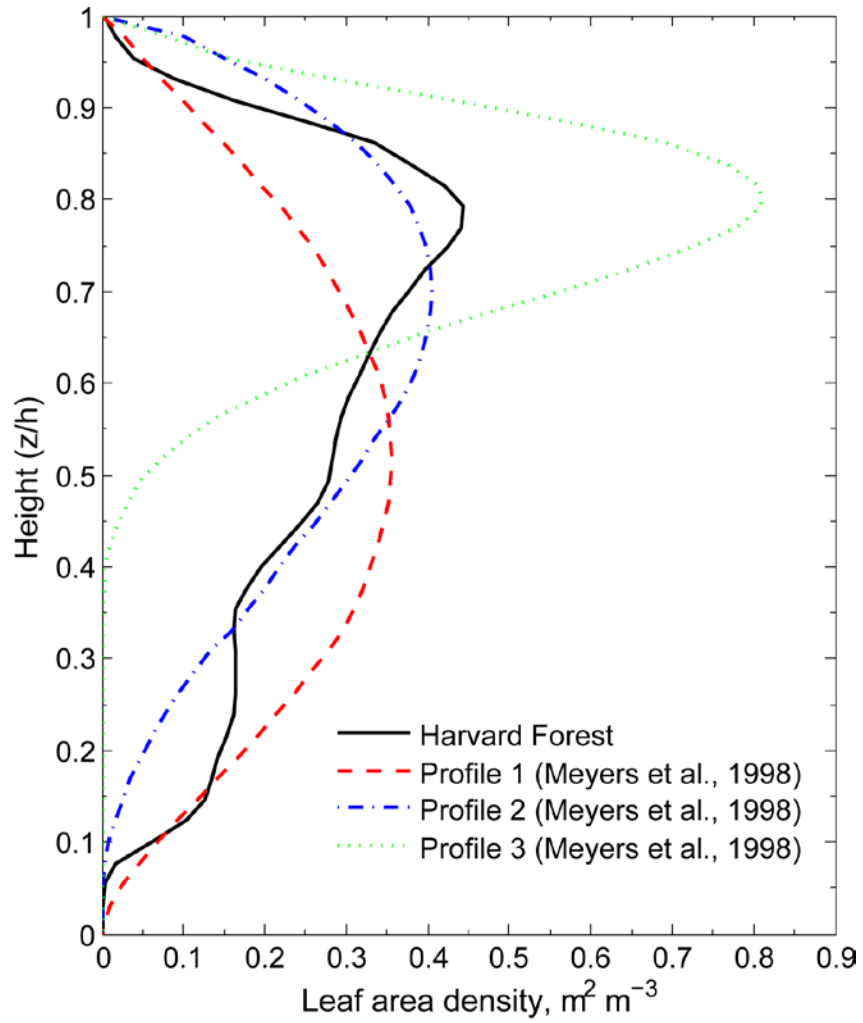


Fig. 7. Vertical profiles of leaf area density in Harvard Forest and those used in sensitivity experiments.